The Reaction $\gamma p \rightarrow \pi^0 \gamma' p$ and the Magnetic Dipole Moment of the $\Delta^+(1232)$ Resonance

M. Kotulla,[1] J. Ahrens,[2] J. R. M. Annand,[3] R. Beck,[2] G. Caselotti,[2] L. S. Fog,[3] D. Hornidge,[2] S. Janssen,[1] B. Krusche,[4]
J. C. McGeorge,[3] I. J. D. McGregor,[3] K. Mengel,[1] J. G. Messchendorp,[1] V. Metag,[1] R. Novotny,[1] M. Pfeiffer,[1] M. Rost,[2]
S. Sack,[1] R. Sanderson,[3] S. Schadmand,[1] and D. P. Watts[3]

[1]*II. Physikalisches Institut, Universität Gießen, D-35392 Gießen, Germany*
[2]*Institut für Kernphysik, Johannes-Gutenberg-Universität Mainz, D-55099 Mainz, Germany*
[3]*Department of Physics and Astronomy, University of Glasgow, Glasgow G128QQ, United Kingdom*
[4]*Department of Physics and Astronomy, University of Basel, CH-4056 Basel, Switzerland*
(Received 4 July 2002; published 16 December 2002)

The reaction $\gamma p \rightarrow \pi^0 \gamma' p$ has been measured with the TAPS calorimeter at the Mainz Microtron accelerator facility MAMI for energies between $\sqrt{s} = 1221$–1331 MeV. The cross section's differential in angle and energy have been determined for the photon γ' in three bins of the excitation energy. This reaction channel provides access to the magnetic dipole moment of the $\Delta^+(1232)$ resonance and, for the first time, a value of $\mu_{\Delta^+} = [2.7^{+1.0}_{-1.3}(\text{stat}) \pm 1.5(\text{syst}) \pm 3(\text{theor})]\mu_N$ has been extracted.

PACS numbers: 13.40.Em, 14.20.Gk, 25.20.Lj

The complex structure of the nucleon is reflected in its rich excitation spectrum. Attempts to unravel the baryon structure have led to an impressive determination of the properties of the nucleon, e.g., polarizabilities, magnetic moments, and more general form factors. Additional and substantial insight in the parton structure of the nucleon has been gained through deep inelastic electron scattering. In contrast to that, the knowledge of the nucleon's excited states is limited to the mass of the lowest resonances and its (iso)spin quantum numbers. However, to test the modeling of internal degrees of freedom of the excited states, measurements of static properties are required. In particular, the properties of the $\Delta(1232)$ resonance are of considerable interest because of its prominent position in the excitation spectrum.

In this context, the magnetic moment is an important observable for testing baryon structure calculations. Different predictions for the magnetic moment were made in several calculations [1–4]. The magnetic moments of the baryon octet (N, Λ, Σ, Ξ) of the SU(3) flavor symmetry classification are known very accurately through spin precession measurements. However, for the decuplet baryons, only $\mu\Omega^-$ has been determined, as the lifetime of the other decuplet members is too short for this technique. If SU(3) flavor symmetry were to hold, the Δ and the nucleon would be degenerate in mass and their magnetic moments related through $\mu_\Delta = Q_\Delta \mu_p$, where Q_Δ is the charge and μ_p the proton magnetic moment. However, structure calculations predict significant deviations from this SU(3) value [1–4].

It has been proposed that the electromagnetic structure of the Δ can be determined by measuring a γ transition within the resonance [5]. This method is depicted in Fig. 1, which shows an energy level diagram with the proton (nucleon) as the ground state and the Δ as the first excited state. The Δ structure can be probed by exciting the proton to a Δ, which then emits a real photon and sub-

sequently decays into a nucleon and a pion. Spin and parity conservation require that the lowest order electromagnetic transition is magnetic dipole ($M1$) radiation. This $\Delta \rightarrow \Delta \gamma'$ amplitude is proportional to μ_{Δ^+} and was recently investigated in theoretical calculations [6–8]. The next allowed multipole is the electric quadrupole ($E2$) transition, but this amplitude vanishes in the limit of zero photon energy because of time reversal symmetry [9]. The $E2/M1$ ratio of the transition amplitude $N \rightarrow \Delta$ has been measured to be very small, approximately 0.025 [10], which leads to the assumption that the quadrupole deformation of the Δ is very small. The magnetic octupole ($M3$) transition is suppressed by two additional powers of photon momentum. Hence, the measurement of the reaction $\gamma p \rightarrow \pi^0 \gamma' p$ provides access to μ_{Δ^+}. Unfortunately this final state can also result from bremsstrahlung radiation of the intermediate Δ and the
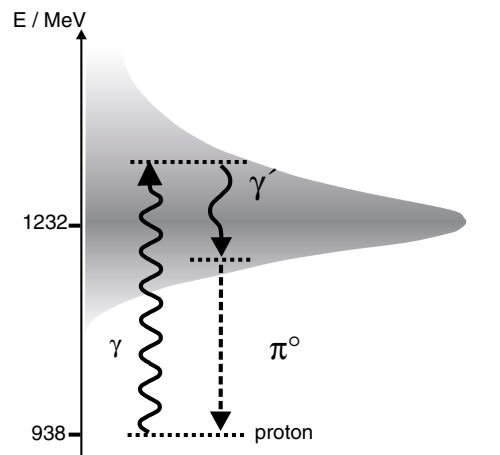

FIG. 1.   Method to study the static electromagnetic properties of the $\Delta^+(1232)$ isobar. The γ' transition carries the information of the magnetic moment of the Δ^+.

proton. These contributions are of the same order as the $\Delta \rightarrow \Delta\gamma'$ transition of interest. Nonresonant contributions are expected to play a minor role, since the partial wave decomposition of the related elastic channel $\gamma p \rightarrow \pi^0 p$ shows the dominance of the Δ resonant reaction process [11]. The reaction channel $\gamma p \rightarrow \pi^+ \gamma' n$ is in that sense less favorable for extracting the magnetic moment of the Δ^+ isobar. An accurate theoretical description of all processes contributing to $\gamma p \rightarrow \pi^0\gamma' p$ is crucial for extracting a precise value for μ_{Δ^+}. The magnetic moment of the Δ^{++} isobar was extracted in a similar way from the reaction $\pi^+ p \rightarrow \pi^+ \gamma' p$. Two experiments at the University of California (UCLA) [12] and the Schweizerisches Institut für Nuklearforschung (SIN, now called PSI) [13] have been performed, and as a result of many theoretical analyses of these data the Particle Data Group [14] quotes a range of $\mu_{\Delta^{++}} = 3.7$–$7.5\mu_N$ (where μ_N is the nuclear magneton). The large uncertainty in the extraction of $\mu_{\Delta^{++}}$ is due to the strong contribution of π^+ bremsstrahlung and model dependencies. In the reaction channel described here, the bremsstrahlung contributions are much weaker.

The reaction $\gamma p \rightarrow \pi^0\gamma' p$ was measured at the electron accelerator Mainz Microtron (MAMI) [15,16] using the Glasgow tagged photon facility [17,18] and the photon spectrometer TAPS [19,20]. A quasimonochromatic photon beam was produced via bremsstrahlung tagging. The photon energy covered the range 205–820 MeV with an average energy resolution of 2 MeV. The TAPS detector consisted of six blocks each with 62 hexagonally shaped BaF_2 crystals arranged in an 8×8 matrix and a forward wall with 138 BaF_2 crystals arranged in a 11×14 rectangle. Each crystal is 250 mm long with an inner diameter of 59 mm. The six blocks were located in a horizontal plane around the target at angles of $\pm54°$, $\pm103°$, and $\pm153°$ with respect to the beam axis. Their distance to the target was 55 cm and the distance of the forward wall was 60 cm. This setup covered $\approx 40\%$ of the full solid angle. All BaF_2 modules were equipped with 5 mm thick plastic detectors for the identification of charged particles. The liquid hydrogen target was 10 cm long with a diameter of 3 cm. Further details are described in [21].

The measurement of the $\gamma p \rightarrow \pi^0\gamma' p$ reaction channel was exclusive since the 4-momenta of all particles in the final state were determined. The π^0 mesons were detected via their two photon decay channel and identified in a standard invariant mass analysis from the measured photon momenta. The two π^0 decay photons and the γ' photon in the final state were distinguished by using the π^0 invariant mass as a selection criterion. The two photons with an invariant mass closest to the π^0 mass were assigned to be the decay photons. The protons were identified using the excellent time resolution of the TAPS detector and the deposited proton energy: The characteristic time of flight dependence on the energy of the proton and a pulse shape analysis [21] were sufficient to identify the proton uniquely. The proton energy calibration was performed by exploiting energy balance of the exclusively measured $\gamma p \rightarrow \pi^0 p$ channel, thereby compensating for the energy loss in the target and plastic detectors. Random TAPS-tagging spectrometer coincidences were subtracted using background events outside the prompt coincidence time window.

Further kinematic checks were performed by exploiting the kinematic overdetermination of the reaction. Special attention had to be paid to background from $2\pi^0$ production arising from events in which one of the four $2\pi^0$ decay photons escaped detection due to the limited solid angle coverage of the detector. In a first step, the conservation of the total momentum was checked in the three Cartesian directions, respectively. After that, a missing mass analysis was performed to discriminate the $2\pi^0$ contamination. The following missing mass was calculated:

$$M_X^2 = [(E_{\pi^0} + E_p) - (E_{\text{beam}} + m_p)]^2 - [(\vec{p}_{\pi^0} + \vec{p}_p) - (\vec{p}_{\text{beam}})]^2, \quad (1)$$

where $E_{\pi^0}, \vec{p}_{\pi^0}, E_p, \vec{p}_p$ denote the energy and momenta of the π^0 and proton in the final state and m_p the proton mass. The resulting distributions (Fig. 2) show two distinct peaks, the widths of which are determined by the detector resolution. The peak near 0.02 GeV^2 reflects the missing mass of a π^0 and therefore originates from the $2\pi^0$ production, while the peak at 0 GeV^2 indicates the missing mass of a photon and hence the $\pi^0\gamma' p$ production. A Monte Carlo simulation of the $2\pi^0$ and $\pi^0\gamma' p$ reactions using GEANT3 [22] reproduces the lineshape of the measured data. The nearly background free identification of the $\gamma p \rightarrow \pi^0\gamma' p$ reaction is demonstrated in Fig. 2. The remaining small $2\pi^0$ background due to the finite detector resolution (16% in the highest energy bin) is subtracted for the cross section determination. Since the information of the photon γ' has not been used for evaluating the missing mass defined in Eq. (1), as another constraint the energy balance $E_{\text{BAL}} = (E_{\text{beam}} + m_p) - (E_{\pi^0} + E_p + E_{\gamma'})$ was calculated [notation as in Eq. (1)]. The energy balance confirms the clean identification of the $\pi^0\gamma' p$ reaction channel.

The cross section was deduced from the rate of the $\pi^0\gamma' p$ events divided by the number of hydrogen atoms per cm^2, the photon beam flux, the branching ratio of π^0 decay into two photons, and the detector and analysis efficiency. The beam flux was determined by counting the scattered electrons in the tagger focal plane and measuring the loss of photon intensity with a 100%-efficient BGO detector which was moved into the photon beam at lowered intensity. The geometrical detector acceptance and analysis efficiency due to cuts and thresholds were obtained using the GEANT3 code and an event generator producing distributions of the final state particles according to [9]. The systematic errors of the efficiency determination are small because the shape of the measured
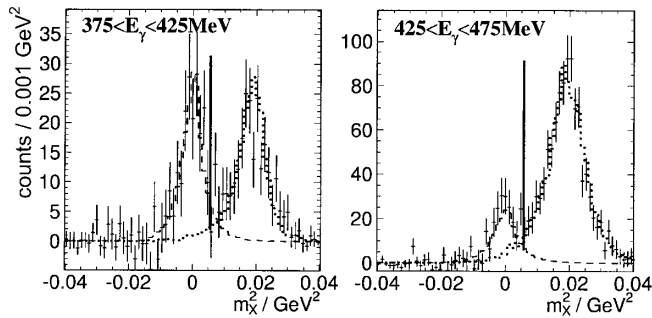
FIG. 2. Missing mass of the $(\pi^0 p)$ system for two beam energies. The peak near 0.02 GeV^2 originates from $2\pi^0$ production and is cut away. The peak at 0 GeV^2 shows the true $\pi^0\gamma' p$ production. The dashed and dotted lines show the corresponding simulated line shapes using GEANT3.

distribution is reproduced by the simulation. The average value for the detection efficiency is 0.25%.

The measured differential cross sections for the reaction $\gamma p \to \pi^0\gamma' p$ are shown in Fig. 3 for three different incident excitation energies $\sqrt{s}$ (i.e., the total γp center of mass energy), starting at the Δ resonance position and going up to 100 MeV above it. The angular distribution of the photon γ' in the c.m. system shows an enhancement for angles around 120°. The energy distribution shifts towards higher γ' energies with rising $\sqrt{s}$, showing an $1/E_\gamma$ form with an additional peak, where the strength and the position depend on the excitation energy $\sqrt{s}$. The different reaction mechanisms suggest such a behavior, where the $1/E_\gamma$ dependence stems from the external bremsstrahlung of the proton in the final state. The position of the peak structure (the energy of γ') originating partly from the Δ radiation is determined by the differ-

ence of $\sqrt{s}$ and the Δ peak mass and a small correction due to the available phase space. The Δ decay mechanism contribution is emphasized, when the energy differential cross section is divided by $1/E_\gamma$ (see Fig. 3).

The first series of calculations, including only the resonant $\Delta \to \Delta\gamma'$ process as indicated in Fig. 1, were done by Machavariani *et al.* [6,7] and Drechsel *et al.* [8]. Both groups use the effective Lagrangian formalism, and in addition the latter group uses a quark model approach to describe the reaction. Since these calculations consider only the Feynman diagram which is sensitive to μ_{Δ^+}, they cannot reproduce the measured cross sections.

Recently, Drechsel and Vanderhaeghen [9] extended their model and included bremsstrahlung diagrams (resonant Δ, nonresonant Born diagrams, and ω exchange). This calculation is shown in comparison to the measured cross sections in Fig. 3. The overall shape is reproduced very well, although the absolute value is overestimated for the highest excitation energy. This is related to an overestimate in the calculation of the reaction $\gamma p \to \pi^0 p$, which is well understood and attributed to πN rescattering contributions [9]. A model independent determination of the $\pi^0\gamma' p$ cross section is feasible in the soft photon limit, which relates $\pi^0\gamma' p$ production to $\pi^0 p$ production in the limit of vanishing photon energy $E_{\gamma'}$ [23]:

$$\lim_{E_{\gamma'}\to 0}\left(\frac{d\sigma}{dE_{\gamma'}}\right) = \frac{1}{E_{\gamma'}}\sigma_0, \qquad (2)$$

$$\sigma_0 = \int d\Omega_{\pi^0}\left(\frac{d\sigma}{d\Omega_{\pi^0}}\right)\frac{2\alpha_{em}}{\pi}\left\{\left(\frac{v^2+1}{2v}\right)\ln\left(\frac{v+1}{v-1}\right)-1\right\},$$

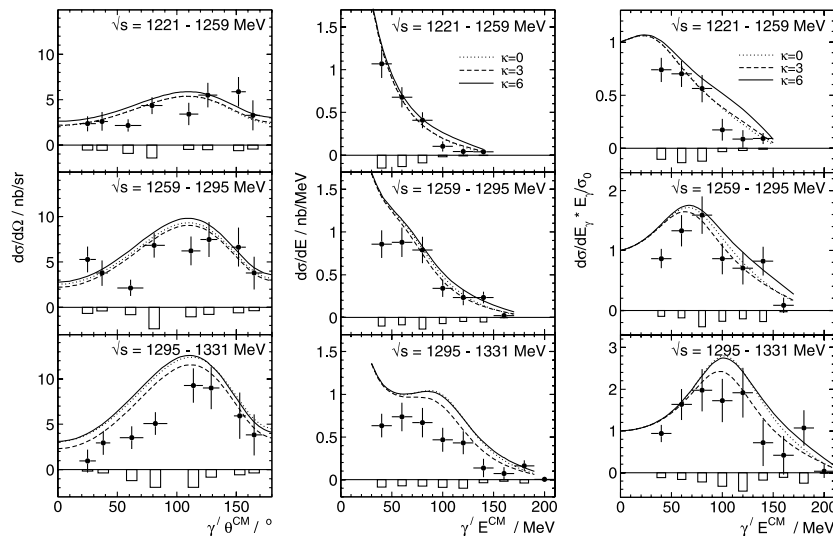$$v = \sqrt{1-\frac{4m_p^2}{t}}, \qquad t = (k-p_{\pi^0})^2.$$

FIG. 3. Differential cross sections for three excitation energies $\sqrt{s}$ in the c.m. frame. Bar chart: systematic errors. Left: angular distribution of the photon γ'. Middle: energy distribution. Lines: calculation [9] for $\kappa_{\Delta^+} = 0$, 3, and 6. Right: energy distribution divided by the soft photon limit $\frac{\sigma_0}{E_\gamma}$, respectively, for the data and the calculation.

$d\sigma/d\Omega_{\pi^0}$ labels the differential cross section for $\pi^0 p$ production, m_p the proton mass, t the four momentum transfer between the initial photon and the π^0 meson, and $\alpha_{em} = e^2/4\pi \approx 1/137$. According to Eq. (2), the energy differential cross section divided by $\sigma_0/E_{\gamma'}$ should be equal to 1 in the limit of zero photon energy $E_{\gamma'}$. This ratio is shown in the right column of Fig. 3, where $d\sigma/d\Omega_{\pi^0}$ in Eq. (2) is calculated with the same effective Lagrangian model [9]. For comparison to the experimental results, the data are also plotted as a cross section ratio where σ_0 has been determined from Eq. (2) using consistently the measured differential cross section $d\sigma/d\Omega_{\pi^0}$ of the $\gamma p \rightarrow \pi^0 p$ reaction. The cross section ratios show better agreement; they are less sensitive to uncertainties in the model calculation as well as uncertainties in the determination of the photon flux and target length. The sensitivity to the magnetic moment of the Δ^+ is illustrated in Fig. 3 by the difference of the three curves. The Δ^+ magnetic moment can be obtained from the anomalous magnetic moment κ_{Δ^+} which is the only free parameter of the calculation [9]

$$\mu_{\Delta^+} = (1 + \kappa_{\Delta^+})\frac{e}{2m_\Delta} = (1 + \kappa_{\Delta^+})\frac{m_N}{m_\Delta}\mu_N, \qquad (3)$$

where $\mu_N = e/2m_N$ is the nuclear magneton. A combined maximum likelihood analysis [14] of the three cross section ratios in Fig. 3 yields a value of $\mu_{\Delta^+} = (2.7^{+1.0}_{-1.3} \pm 1.5)\mu_N$; the goodness of fit is $\chi^2/F = 1.8$ ($F = 21$). The first error represents the statistical uncertainty, and the second one reflects the systematic errors given in Fig. 3. This error does not include the systematic error of the model calculation which is of the order of $\pm 3\mu_N$, estimated from the uncertainties discusssed in [9]. The extracted value of μ_{Δ^+} is in the range of different baryon structure calculations [1–4], but not sensitive enough to discriminate between them.

In conclusion, we have made the first measurement of the magnetic moment of the $\Delta^+(1232)$ resonance by exploiting the reaction $\gamma p \rightarrow \pi^0 \gamma' p$. We see a clear deviation from a soft bremsstrahlung cross section at higher energies of the radiated photon, pointing to a sentitivity to the magnetic moment of the $\Delta^+(1232)$ resonance. However, the limited statistics and the uncertainty of the model lead to a value of the $\Delta^+(1232)$ magnetic moment, which is not sufficiently precise for a detailed test of different baryon structure calculations. This situation calls for a follow-up experiment with much higher statistical precision, so that the kinematic regions most sensitive to μ_{Δ^+} can be exploited [9,24]. An investigation of the cross section asymmetry using a polarized photon beam would also be valuable. To supplement, an improvement in the theoretical description is necessary to minimize the model dependence. The measurement can be extended to higher excited states of the nucleon. In particular, the magnetic moment of the $S_{11}(1535)$ resonance is accessible via the reaction $\gamma p \rightarrow \eta \gamma' p$ because of its clean distinction from other resonances in the second resonance region through the η decay channel.

[1] D. Leinweber, T. Draper, and R. Woloshyn, Phys. Rev. D **46**, 3067 (1992).
[2] M. Butler, M. Savage, and R. Springer, Phys. Rev. D **49**, 3459 (1994).
[3] H. Kim, M. Praszalowicz, and K. Goeke, Phys. Rev. D **57**, 2859 (1998).
[4] T. Aliev, A. Özpineci, and M. Savci, Phys. Rev. D **62**, 053012 (2000).
[5] L. Kontratyuk and L. Ponomarev, Yad. Fiz. **7**, 11 (1968) [Sov. J. Nucl. Phys. **7**, 82 (1968)].
[6] A. Machavariani, A. Faessler, and A. Buchmann, Nucl. Phys. **A646**, 231 (1999).
[7] A. Machavariani, A. Faessler, and A. Buchmann, Nucl. Phys. **A686**, 601 (2002).
[8] D. Drechsel *et al.*, Phys. Lett. B **484**, 236 (2000).
[9] D. Drechsel and M. Vanderhaeghen, Phys. Rev. C **64**, 065202 (2001).
[10] R. Beck *et al.*, Phys. Rev. Lett. **78**, 606 (1997).
[11] D. Drechsel, O. Hanstein, S. Kamalov, and L. Tiator, http://www.kph.uni-mainz.de/MAID (2000).
[12] B. Nefkens *et al.*, Phys. Rev. D **18**, 3911 (1978).
[13] A. Bosshard *et al.*, Phys. Rev. D **44**, 930 (1991).
[14] D. Groom *et al.*, Eur. Phys. J. C **15**, 1 (2000).
[15] T. Walcher, Prog. Part. Nucl. Phys. **24**, 189 (1990).
[16] J. Ahrens *et al.*, Nucl. Phys. News **4**, 5 (1994).
[17] I. Anthony *et al.*, Nucl. Instrum. Methods Phys. Res., Sect. A **301**, 230 (1991).
[18] S. Hall *et al.*, Nucl. Instrum. Methods Phys. Res., Sect. A **368**, 698 (1996).
[19] R. Novotny, IEEE Trans. Nucl. Sci. **38**, 379 (1991).
[20] A. R. Gabler, Nucl. Instrum. Methods Phys. Res., Sect. A **346**, 168 (1994).
[21] R. Novotny *et al.*, IEEE Trans. Nucl. Sci. **43**, 1260 (1996).
[22] R. Brun *et al.*, GEANT3 User's Guide, CERN, Data Handling Division DD/EE/84-1 (1986).
[23] W.-T. Chiang *et al.*, nucl-th/0211061.
[24] M. Kotulla, Acta Phys. Pol. B **33**, 957 (2002).